# Optical absorption of ion-beam sputtered amorphous silicon coatings

Jessica Steinlechner, Iain W. Martin, Riccardo Bassiri, Angus Bell, Martin M. Fejer, Jim Hough, Ashot Markosyan, Roger K. Route, Sheila Rowan, and Zeno Tornasi

Phys. Rev. D **93**, 062005 — Published 25 March 2016

DOI: 10.1103/PhysRevD.93.062005

# Optical Absorption of Ion-Beam Sputtered aSi Coatings

Jessica Steinlechner,[1] Iain W Martin,[1,*] Riccardo Bassiri,[2] Angus Bell,[1] Martin M. Fejer,[2] Jim Hough,[1] Ashot Markosyan,[2] Roger K. Route,[2] and Sheila Rowan[1]

[1] *SUPA, School of Physics and Astronomy, University of Glasgow, Glasgow, G12 8QQ, Scotland*
[2] *E.L. Ginzton Laboratory, Stanford University, Stanford, California 94305, USA*

Low mechanical loss at low temperatures and a high index of refraction should make silicon optimally suited for thermal noise reduction in highly-reflective mirror coatings for gravitational wave detectors. However, due to high optical absorption, amorphous silicon (aSi) is unsuitable for being used as a direct high-index coating material to replace tantala. A possible solution is a multi-material design, which enables exploitation of the excellent mechanical properties of aSi in the lower coating layers. The possible number of aSi layers increases with absorption reduction. In this work, the optimum heat treatment temperature of aSi deposited via ion-beam sputtering was investigated and found to be 450 °C. For this temperature, the absorption after deposition of a single layer of aSi at 1064 nm and 1550 nm was reduced by more than 80 %.

PACS numbers: 42.25.Bs, 42.79.Wc

## I. INTRODUCTION

On 14th of September 2015 the first gravitational wave signal was directly detected by the Advanced LIGO gravitational wave detectors (GWDs) [1], which are large-scale Michelson-type interferometers with arms of order of several kilometers in length. In such detectors, laser interferometry is used to measure changes in the relative separation of suspended test-masses, which are coated to form highly reflective (HR) mirrors. The 1st and 2nd generations of GWDs operate at room temperature, using a laser wavelength of 1064 nm. Future, more sensitive detectors such as upgrades to *Advanced LIGO* [2] and the low frequency detector within the *Einstein Telescope* (ET) [3, 4] may be operated at cryogenic temperatures to reduce thermal noise. The presently used test-mass material fused silica becomes unsuitable at low temperatures due to high mechanical loss and thus high thermal displacement noise [5]. A promising replacement material with low mechanical loss at cryogenic temperatures is crystalline silicon (cSi) [6, 7]. cSi has several other interesting properties including zero crossings of the thermal expansion coefficient at 120 K and 20 K resulting in low thermo-elastic noise [8, 9] and a low optical absorption at the telecommunication wavelength of 1550 nm [10, 11].

The optical requirements for the end test masses for ET are a high reflectivity (transmission = 5 ppm) and low optical absorption of about 1 ppm [3]. In addition, low coating thermal noise is necessary, which can be achieved by reducing coating mechanical loss, reducing coating thickness or by utilizing larger beam sizes on the detector mirrors [14]. Currently, the 2nd generation detectors use coating stacks consisting of alternating layers of silica ($SiO_2$) and tantala ($Ta_2O_5$), but both materials show increasing mechanical loss when being cooled to low temperatures [12, 13]. To achieve the ET requirements, coating thermal noise has to be further reduced by reducing the mechanical loss and/or the thickness of the coating. The high reflectivity of a coating is achieved by using alternating layers with a high index of refraction $n_1$ and a low index of refraction $n_2$, and an optical thickness $n \times t$ (where $t$ is the geometric thickness of the layer) of a quarter of a wavelength. With increasing $\Delta n = |n_2 - n_1|$ the reflectivity at each layer boundary increases and consequently a smaller number of layers required to achieve high reflectivity. Additionally, the geometric thickness of the layers decreases with increasing refractive index. Thus to minimize coating thermal noise a material of high refractive index and low mechanical loss is desirable. In comparison to tantala, amorphous silicon (aSi) shows low mechanical loss at low temperatures [15] and has a high index of refraction which would both result in a significant thermal noise reduction, if aSi was used for the high-index layers of a mirror coating.

The optical absorption of aSi-based HR coatings deposited by *ion plating* has been shown to be approximately 1000 ppm at 1550 nm [16] and therefore too high for use in mirror coatings using a design of two alternating high and low refractive materials. However, a multi-material design, in which the outermost bilayers are made of $Ta_2O_5$ and $SiO_2$ to significantly reduce the incident laser power, while in the lowest bilayers the $Ta_2O_5$ is replaced by aSi, enables exploitation of the low mechanical loss and high refractive index of aSi to reduce the thermal noise at 20 K by 25 % while keeping the optical absorption as low as 5 ppm [17, 18].

While ion plating aSi coatings show some promise as part of a multi-material design, lower absorption is needed to meet the ET requirements for thermal noise. In addition, other crucial parameters of ion plating coatings, including mechanical loss, scattering and homogeneity, have not yet been investigated.

This paper presents absorption measurements on an aSi single layer and an aSi/$SiO_2$ bilayer produced with the *ion-beam sputtering* (IBS) deposition technique, which is currently used for coatings in GWDs as it pro-

* iain.martin@glasgow.ac.uk

vides low scattering and high homogeneity. The mechanical loss of these coatings at 10 K, which is the ET design temperature, has previously been shown to be a factor of 40 lower than the loss of $Ta_2O_5$ [19]. The absorption of these coatings was measured at 1064 nm and 1550 nm for heat treatment of up to 1000 °C, in air and in vacuum and the optimal temperature and duration was investigated. Further, the expected coating performance at cryogenic temperatures was investigated by carrying out temperature dependent optical absorption measurements.

## II. OPTICAL ABSORPTION MEASUREMENTS

The effect of heat treatment on optical absorption of coatings containing aSi was investigated by using a 500 nm aSi single layer and a bilayer of 112 nm aSi with 267 nm $SiO_2$ on top, which corresponds to optical thicknesses of a quarter of a wavelength (QWL) at 1550 nm. Both coatings were made by *Advanced Thin Films* (ATF) [20] using IBS, and were deposited on fused silica substrates. Figure 1 shows the two coating designs.

The absorption of the coatings was measured using photothermal common-path interferometry (PCI) [21]. Section II A briefly describes the method. In Sec. II B absorption results are presented for the aSi single layer (Sec. II B 1) and the bilayer (Sec. II B 2) and the results are compared (Sec. II B 3). Section II C investigates the effect of the heating time on absorption, and Sec. II D a possible intensity dependence of the optical absorption of the bilayer. The homogeneity of the bilayer coating is shown in Sec. II E by mapping a 3 mm × 5 mm area. In Sec. II F the temperature dependence of the absorption of a bilayer between room temperature and 30 K is presented.

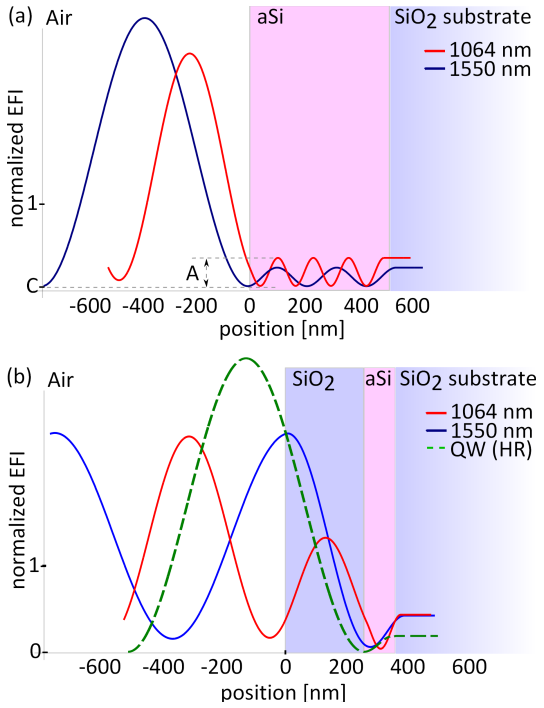


FIG. 1. (a) Normalized EFI inside the aSi single layer (pink) on a fused silica substrate at 1064 nm (red) and 1550 nm (blue). The optical thickness of the aSi layer as deposited was determined by a reflectivity measurement to be 1905 nm (= 500 nm x 3.81) at 1550 nm and 2030 nm (= 500 nm x 4.06) at 1064 nm. (b) EFI inside the aSi/$SiO_2$ bilayer ($SiO_2$ in blue, aSi in pink) on a fused silica substrate for measured optical thickness of the aSi layer of 433 nm (= 112 nm x 3.87), while for the $SiO_2$ layer design parameters of 267 nm and n=1.45 were used. The dashed green line shows the EFI for an optimal QWL of aSi (ignoring the $SiO_2$ layer on top) as being used in HR coatings.

### A. Photothermal common-path interferometry

The photothermal common-path interferometry measurement technique [21] uses a strong pump laser beam with small waist (high intensity) to create a thermally induced optical length change in a substrate either by direct absorption or, in this case, by the absorption in a coating applied to the substrate. A weak probe beam, larger in diameter than the pump beam, crosses the pump beam so that only the overlapping portion of the probe beam is affected by the optical length change and is phase shifted. Interference between the phase shifted and non phase shifted portion of the probe beam creates a signal which is directly proportional to the absorption. The pump beam is amplitude modulated. A lock-in amplifier is used to recover the absorption signal at the modulation frequency and also provides information about the phase of the signal with reference to the pump modulation. The parameters of the pump beam and the thermal diffusion in the thermally affected material determine this phase.

Figure 2 shows typical measurements of the amplitude (a) and the phase (b) for the aSi single layer (purple, dashed line) and the bilayer (green line). The measured signal was calibrated by using a fused silica neutral density filter (FSQ-ND02 from Newport [24]) with a coating absorption of 21.4 % and a phase of about -65 ° at the pump modulation frequency of 407 Hz. For the aSi coated fused silica substrates, the phase is expected to be very similar to the calibration substrate phase, but the measurements show a slightly different phase for the bilayer of -58 ° and a phase of -48 ° for the aSi single layer. In Fig. 2(b) it also can be seen that the aSi single layer amplitude signal shows higher side maxima than the bilayer. The phase deviation and differing amplitude shape indicate a contribution not only of the fused silica substrate, as it is usually the case for amorphous coatings, but also of the aSi coating to the absorption signal. Therefore the measured absorption was recalibrated considering the contribution of the aSi. A detailed description of this procedure can be found in [22]. The absorption results presented in the following sections have been

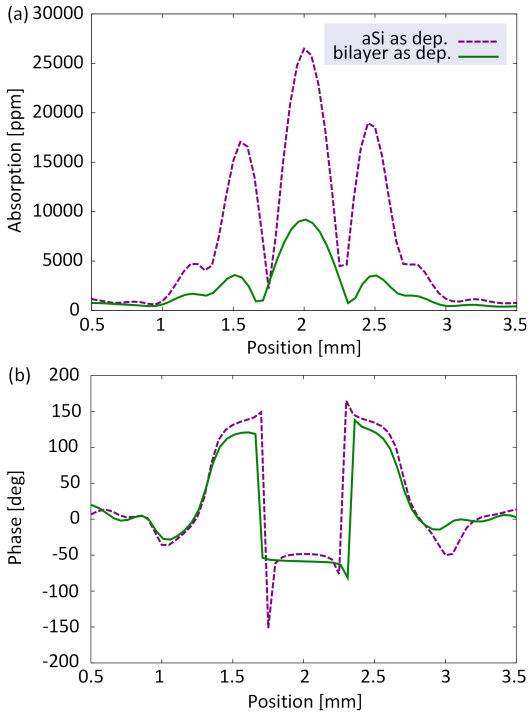


FIG. 2. (a) Photothermal common-path interferometry absorption scans of the aSi single layer (purple, dashed line) and the aSi/$SiO_2$ bilayer (green line) as deposited at 1550 nm (before recalibrating the aSi single layer signal and normalizing the EFI to optimal QWLs). (b) Phase of the aSi single layer and the bilayer as deposited. The x axis shows the position of the coating, which is moved relative to the beam crossing point. At 2 mm the beam crossing point is on the coating and the signal maximizes.

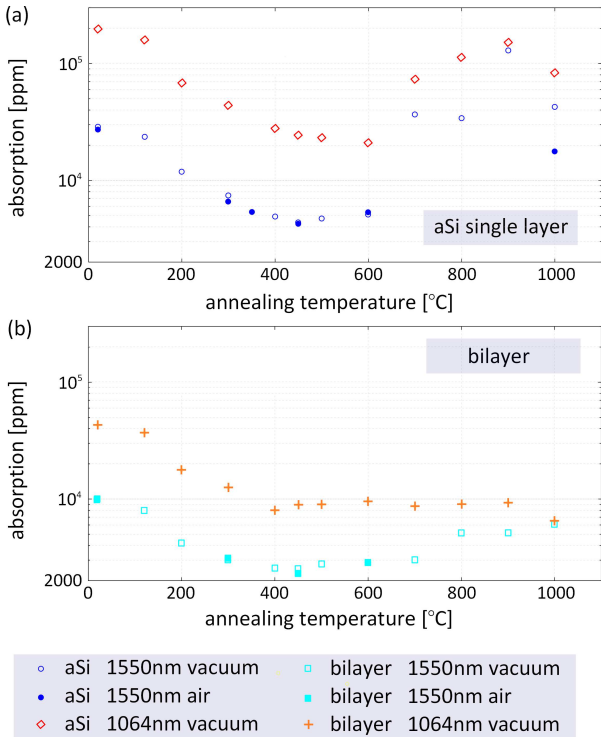


FIG. 3. Absorption measured for different heat treatment at temperatures up to 1000 °C: The absorption was measured for (a) the aSi single layer and (b) for the bilayer.

recalibrated based on the phase information.

During the measurements, the calibration was routinely checked. For a change of more than 10 % due to misalignment (drift of alignment components) the measurements were repeated. This 10 % error dominates errors from power meter uncertainties, laser power fluctuations during the measurements, and discrepancies of the results after realignment. As these errors are uncorrelated, for all measurements, error bars of ±10 % are assumed.

### B. Absorption results for heat treatment at different temperatures

#### 1. *Absorption of the aSi single layer coating*

The aSi single layer coatings 500 nm in thickness were heated in vacuum (pressure < 0.1 mbar) to temperatures of up to 1000 °C. One sample was heated to 120 °C. A second sample was used for further heat treatment from 200 to 1000 °C in steps of 100 °C. Around 450 °C the step size was reduced to 50 °C. After heating, all samples were allowed to cool naturally in the environment in which they had been heated. The absorption was measured at 1550 and at 1064 nm. The absorption results are presented in Fig. 3(a), where the blue, empty circles (○) show the absorption 1550 nm, and the red diamonds (◇) the absorption at 1064 nm. For the measurements at 1550 and 1064 nm the same samples were used.

For some temperatures, comparisons are made to samples which were heat treated in air. The filled circles (●) show absorption results for heat treatment in air and in an unknown environment (heat treatment by ATF after deposition for 300 and 450 °C). For temperatures of 350, 600, and 1000 °C, samples were heated from an as-deposited state to the final temperature for 3 hrs. Note that the results which are assigned to 20 °C (room temperature) mean no further heat treatment after deposition, but the deposition temperature was above room temperature.

For temperatures up to 600 °C, the absorption results for heat treatment in air and in vacuum are in good agreement. Only the absorption for 1000 °C heat treatment is significantly lower for heating in air than for heating in vacuum, which most likely is a result of very inhomogeneous absorption on different positions of the coating for heat treatment at temperatures above 900 °C. For all temperature steps, the absorption at 1550 nm is clearly lower than at 1064 nm.

The absorption measured depends on the thickness of the coating, and on the EFI in the layer changing the

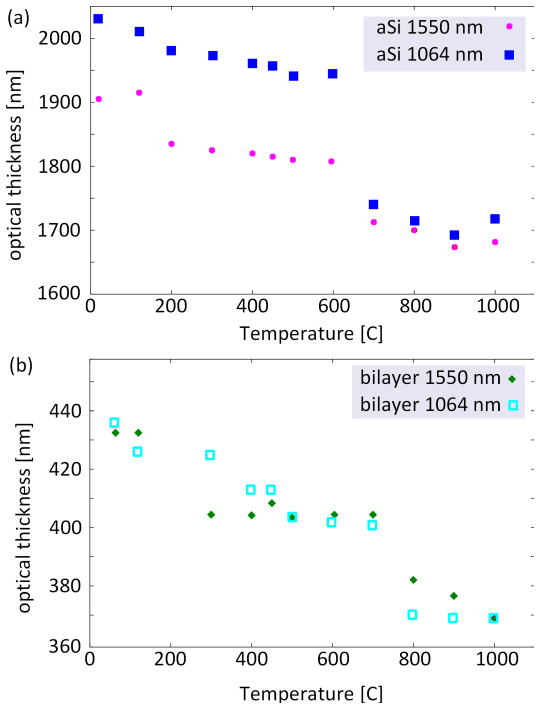


FIG. 4. Development of the optical thickness with heat-treatment temperature, calculated based on transmission measurements, for (a) the aSi single layer and (b) the bilayer coating, at 1550 nm and at 1064 nm. Note the 'steps' in optical thickness, which are discussed in Sec. II B 3.

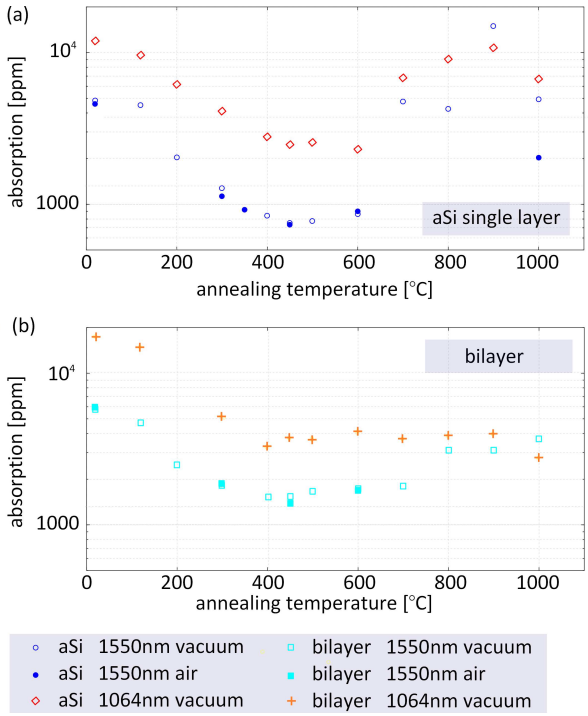


FIG. 5. Absorption results from Fig 3 after normalisation to QWLs: (a) for the aSi single layer and (b) for the bilayer, both at 1550 nm and at 1064 nm.

power inside the layer which can be absorbed. For making corrections regarding changes of the optical thickness during heat treatment and to allow comparison of the absorption of the aSi single layer to a highly-reflective multi-layer coating, the absorption results are normalized to a thickness of a QWL.

The EFI inside a thin coating layer depends on the wavelength and the optical thickness $n \times t$, and minimizes for a thickness of $(2N+1)$ QWLs (where the reflectivity maximizes). Therefore the measured absorption of our non-QWL coatings has to be scaled to make it comparable to what can be expected in an HR coating.

For each temperature step the input laser power and the transmitted laser power were measured. Considering the absorption and reflection at the back face of the fused silica substrate, the reflection was calculated. The optical thickness $t \times n$ of the coatings was calculated using a coating simulation program [23] based on matrix transfer formalism. Figure 4(a) shows the development of the optical thickness with heat-treatment temperature for the aSi single layer at 1550 nm and at 1064 nm indicating an optical thickness decrease with increasing temperature. Assuming the design thickness of 500 nm for the aSi single layer coating as deposited to be accurate, the measurements of the optical thickness correspond to refractive indices of $n_{1550\mathrm{nm}} = 3.81$ and $n_{1064\mathrm{nm}} = 4.06$.

Based on the measurements of the optical thickness, the EFI for the coatings was simulated using [23]. Due to non-perfect QWLs, the EFI differs significantly from an optimal HR coating stack. Figure 1(a) shows the EFI at 1064 nm (red) and at 1550 nm (blue) inside the 500 nm aSi single layer (pink).

The EFI in our coatings is a function of the form $\sin^2(\mathrm{x})$ with amplitude $A$ and an offset $C$ (see Fig. 1(a)). Integrating over the coating thickness $t$ results in a total intensity of

$$I_{\mathrm{coating}} = \frac{A}{2}(t - \sin(t)\cos(t)) + Ct\,. \qquad (1)$$

A possible shift of the sin minimum relative to the coating surface was considered additionally. For a QWL, $C$ disappears and $A$ optimizes to a minimum. The expected absorption $\alpha_{\mathrm{QWL}}$ was therefore multiplied with a scaling factor $I_{\mathrm{QWL}}/I_{\mathrm{coating}}$ to normalize the absorption to QWL equivalent thickness.

The absorption results presented in Fig. 3(a) were scaled to the expected intensity in a QWL in an HR coating (112 nm at 1550 nm and 77 nm at 1064 nm) and are shown in Fig. 5(a). The symbols are identical to the symbols used in Fig. 3. Table I lists the results which are shown in Fig. 5. At 1550 nm the aSi single layer has an absorption minimum for heat treatment at a temperature of 450 °C. At this temperature also a significant decrease of up to a factor of 4 in mechanical loss was observed following heat-treatment of an as-deposited coating [19].

TABLE I. Final absorption results (normalized to the absorption which can be expected in QWLs in an HR coating) for the aSi single layer and bilayer at 1550 nm and for the aSi single layer at 1064 nm for heat treatment in air and in vacuum at different temperatures.

| | vacuum 1550 nm | | air 1550 nm | | vacuum 1064 nm | |
|---|---|---|---|---|---|---|
| | aSi | bilayer | aSi | bilayer | aSi | bilayer |
| Temp. [°C] | absorption [ppm] | | | | | |
| 20 | 4830 | 5608 | 4562 | 5966 | 11928 | 16566 |
| 120 | 4541 | 4427 | | | 9590 | 14161 |
| 200 | 2035 | 2361 | | | 6172 | |
| 300 | 1274 | 1633 | 1223 | 1868 | 4096 | 4838 |
| 350 | | | 916 | | | |
| 400 | 843 | 1430 | | | 2787 | 3077 |
| 450 | 755 | 1453 | 730 | 1390 | 2469 | 3528 |
| 500 | 776 | 1609 | | | 2551 | 3547 |
| 600 | 860 | 1591 | 897 | 1692 | 2302 | 3858 |
| 700 | 4757 | 1670 | | | 6804 | 3499 |
| 800 | 4254 | 2961 | | | 9048 | 3663 |
| 900 | 14914 | 2961 | | | 10728 | 3768 |
| 1000 | 4906 | 3445 | 2033 | | 6691 | 2624 |

### 2. *Absorption of the aSi/$SiO_2$ bilayer coating*

Together with the aSi single layer coatings, bilayer samples were heat treated at each temperature step. The absorption measurement and calibration procedure was equivalent to the aSi single layer. The absorption results are presented in Fig. 3(b). The light blue, empty squares (□) show the absorption of the bilayer at 1550 nm. The orange pluses (+) represent the bilayer absorption at 1064 nm. Again, for the measurements at 1550 and 1064 nm the same samples were used. The filled squares (■) show absorption results for heat treatment in air and in an unknown environment. The absorption results for heat treatment in air and in vacuum are in good agreement. Like for the aSi single layer, for the bilayer the absorption at 1550 nm is clearly lower than at 1064 nm. The absorption of a $SiO_2$ single layer 500 nm in thickness was also measured. This layer shows an absorption which is negligible (25 ppm for a 500 nm layer, before heat treatment) compared to the absorption of the aSi layers and suggests that the absorption of the bilayer is likely to be dominated by the aSi component.

The development of the optical thickness with heat-treatment temperature for the aSi component of the bilayer at 1550 nm and at 1064 nm is shown in Fig. 4(b). This information was used to simulate the EFI in the bilayer. Figure 1(b) shows the EFI inside the bilayer ($SiO_2$ in blue, aSi in pink) at 1064 nm (red) and at 1550 nm (blue). The thickness of each layer is a QWL at 1550 nm. Note that in our bilayer the order of the high and low index materials is reversed compared to an HR coating which starts with an high index QWL to maximize the reflectivity. Therefore, the EFI in our bilayer is different from the EFI in an HR coating bilayer. The dashed green line in Fig. 1(b) shows the EFI for an optimal QWL of aSi as it is used in a HR coating design (ignoring the $SiO_2$ layer), which is significantly lower than the EFI in our bilayer.

The absorption results presented in Fig. 3(b) were scaled to the expected intensity in a QWL in an HR coating in the same way as for the aSi single layer, which the final absorption results being shown in Fig. 5(b) using identical symbols to those used in Fig. 3. Table I lists the results which are shown in Fig. 5. Very similar to the aSi single layer, at 1550 nm the bilayer shows an absorption minimum for heat treatment at a temperature of 400 °C.

### 3. *Comparison of the results for the aSi single layer and the bilayer*

While the absorption of the aSi single layer and the bilayer at 1550 nm is almost identical for low heat treatment temperatures (120 and 200 °C), the absorption minimum around 400 °C is a factor of two higher for the bilayer. The higher absorption of the bilayer compared to the aSi single layer is unlikely to be caused by the $SiO_2$ layer, as this is insignificant in absorption (25 ppm for 500 nm of $SiO_2$ before heat treatment). That the overall shape of the curve is much less distinct for the bilayer (e.g. the absorption 'peak' at 800/900 °C is missing) might indicate that it is affected less significantly by the heat treatment than the single layer, possibly by the $SiO_2$ layer restricting the aSi performance. This might be related to an effect shown in nano-layer coatings, which are more resistant to crystallization due to heat treatment (compared to thicker layer structures) [25].

This is also indicated by the step-like absorption increase which can be seen in Fig. 5 between 600 and 700 °C for the aSi single layer (a). This 'step' is shifted to a higher temperature (between 700 and 800 °C) for the bilayer (b). The same shifted step occurs for the optical thickness, which is shown in Fig. 4. (Note that the absorption step already exists in the non-normalized absorption measurement, Fig. 3, and therefore is independent from the recalibration based on the optical thickness measurement.) The optical thickness measurements show another 'step' for the aSi single layer between 120 and 200 °C at 1550 nm. This step is less distinct at 1064 nm. A failed measurement point in the optical thickness measurement for the bilayer prevents a comparison of the aSi single layer and bilayer.

The bilayer is closer to the design of a highly-reflective multi-layer coating of interest for application in GWDs. In an aSi/$SiO_2$ HR coating, the absorption contribution of the layers below the first bilayer to the total coating absorption is approximately 40 %. Applying the result for the aSi single layer at 1550 nm at the optimal heat treatment temperature of 450 ° to a full HR stack, therefore would result in an expected absorption of $1.4 \times 755\,\text{ppm} = 1057\,\text{ppm}$. The absorption for an

TABLE II. Absorption of the bilayer at 1550 nm for different times of heat treatment. The two results for sample (b) and (f) were measured on different positions on the samples. (Results not normalized to QWLs.)

| sample | heat treatment temperature | environment | result [ppm] |
|---|---|---|---|
| (a) | by ATF at 450 °C (time unknown) | unknown | 2289 |
| (b) | by us for 3 hrs at 450 °C | air | 2396 |
| | | | 2368 |
| (c) | by us for 3 hrs at 450 °C | air | 2350 |
| | (previously by ATF at 300 °C) | | 2320 |
| (d) | identical to sample (c) + 3 hrs at 450 °C | air | 2260 |
| (e) | by us for 15 min at450 °C | air | 2355 |
| (f) | by us for 1 hr at 450 °C | vacuum | 2347 |
| | (previously heated to 200 °C, 300 °C, 400 °C, 1 hr each) | | 2532 |

HR stack based on the result for the bilayer would be 2002 ppm.

### C. Effect of the time of heat treatment

In this Section measurements of the influence of the time of heat treatment on the bilayer absorption at 1550 nm are presented. The time for a temperature of 450 °C was varied to check that the previously presented absorption results do not significantly change either due to time of heat treatment or due to previous annealing of the coatings to lower temperatures.

Sample (a) was annealed by ATF after deposition to 450 °C. We had no infomation about the annealing parameters such as time and environment for this sample. Sample (b) was annealed by us from an as deposited state for three hours to 450 °C in air. Sample (c) was previously heat treated by ATF to 300 °C (no information about parameters) and afterwards heat treated for three hours in air to 450 °C. Sample (d) is identical to sample (c), but heat treated for a second time for three hours at 450 °C in air. For sample (e) the heat-treatment time was significantly shortened to 15 min. Sample (f) was heat treated in vacuum for 1 hr each to 200, 300, 400, and 450 °C. An overview of the absorption results is shown in Fig. 6. The two results for samples (b), (c) and (f) were measured at different positions. The pink box indicates a deviation of ±10 % from the average result. No significant variation of the absorption was observed for any of the annealing regimes tested. However, it should be noted that the coatings showed a change in colour for an increase of heat-treatment temperature. After heat treatment of sample (d) for 15 min at 600 °C a non-uniform change in colour (less change towards the sample edges) indicated that the sample was not heated through completely.

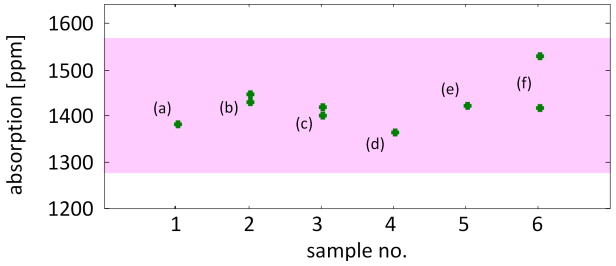


FIG. 6. Absorption at 1550 nm of the bilayer after heat treatment at 450 °C for different times, which can be found in table II. The pink bar indicates boundaries of ±10 % from the mean value of all measurements. (These results are not normalized to QWLs.)

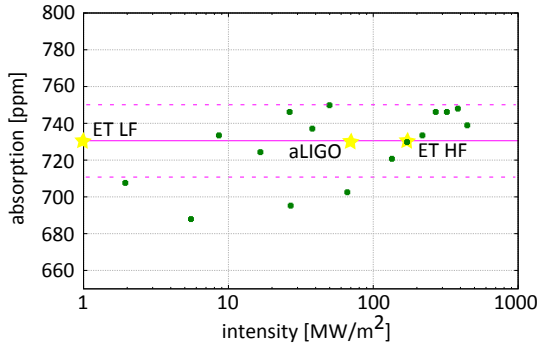


FIG. 7. Dependence of the absorption at 1550 nm of the aSi single layer which was heat treated at 450 °C (pink dots) on the pump beam intensity. The intensity was varied from 2 up to 525 MW/m$^2$. The pink line indicates the mean value of 731 ppm with a standard deviation of 20 ppm (±2.7 %, dashed pink lines).

### D. Intensity dependence of the optical absorption

In cSi two photon absorption causes a non-linear increase of the optical absorption with laser light intensity at 1550 nm [26].

In this Section absorption measurements at 1550 nm are presented for varied pump beam intensity between $P = 4.4$ mW and $P = 1$ W. Figure 7 shows the measured absorption on an aSi single layer coating which was heat treated at 450 °C. For an intensity range from $I = P/\pi w_0^2 = 2$ MW/m$^2$ to 525 MW/m$^2$, which covers the intensities planned for *Advanced LIGO* (71 MW/m$^2$) and ET (0.7 MW/m$^2$ for *ET Low Frequency*, 184 MW/m$^2$ for *ET High Frequency*), no non-linear absorption increase was found. The mean value of 16 measurements at varied intensity was 731 ppm with a standard deviation of 20 ppm (which corresponds to ±2.7 %). Therefore, the results presented in this paper are not affected by non-linear absorption effects.

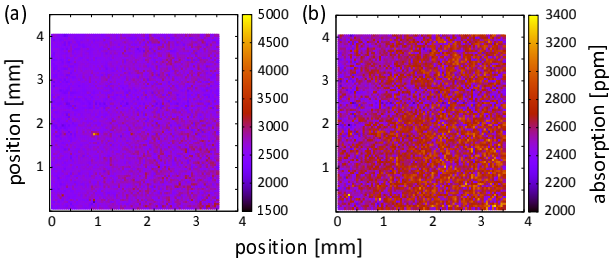


FIG. 8. Surface scan of the absorption at 1550 nm of an aSi/$SiO_2$ bilayer for heat treatment at 450 °C. (a) shows a scan of a 4 mm × 4 mm in steps of 50 $\mu$m (b) shows the same measurement but the high absorbing spots were removed to achieve a better resolution. (Results not normalized to QWLs.)

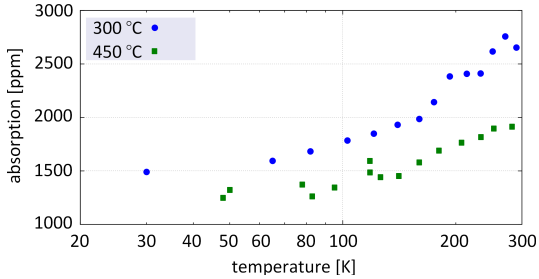


FIG. 9. Optical absorption at 1550 nm of aSi/$SiO_2$ bilayers which were heat treated at 300 and 450 °C as a function of the environmental temperature: The absorption decreases by 45 % when cooling the 300 °C heat treated coating from room temperature to 30 K, and by 35 % when cooling the 450 °C heat treated coating from room temperature to 48 °C. (Results not normalized to QWLs.)

### E. Homogeneity of the optical absorption

To check the homogeneity of the absorption after heat treatment, an area of 4 mm × 4 mm of the 450 °C heat treated bilayer was mapped at a wavelength of 1550 nm.

Measurements were taken in steps of 50 $\mu$m, which causes a small overlap of the measurement positions for the laser beam which is 70 $\mu$m in diameter. In total, approximately 6500 measurements were made on this 16 $mm^2$ area. Figure 8(a) shows the map of the measured absorption indicating homogeneity with a few high absorbing spots. (These spots might originate from dust/non-perfect cleaning.) Figure 8(b) shows the same measurement but the high absorbing spots were removed to achieve a better resolution for the remaining results on the coatings to ensure no strong variations of the absorption. The mean value and standard deviation of the optical absorption is (2640 ± 227) ppm. We conclude that the absorption at the optimal heat-treatment temperature of 450 °C is homogeneous. For higher temperatures of 800 °C and above the absorption of the coatings varies significantly. An aSi single layer after heat treatment at 1000 °C showed a mean value and standard deviation for the absorption of (3.88 ± 1.02) %.

### F. Temperature Dependence of the Optical Absorption

The low-temperature absorption measurements were carried out in a temperature range of 30 to 300 K, where the samples were situated inside a flow cryostat under vacuum. Two thermosresistors were attached to the top and bottom of the sample and the measurements started after the difference in their readings was less than 5 K for each temperature step.

The temperature dependence of the optical absorption at 1550 nm is shown in Fig. 9 for an aSi/$SiO_2$ bilayer heat treated at 300 and 450 °C. The absorption decreases monotonically from room temperature to the lowest temperature reached. It is also apparent that the 450 °C heat treated sample exhibits lower absorption than the 300 °C heat treated sample across the entire temperature range.

Since the absorption of the $SiO_2$ layer is negligible as stated in Sec. II A, one can assume that the absorption of the bilayer samples is caused predominantly by the aSi layer. Therefore the observed temperature variation of the absorption can also be attributed to the aSi layer. From Fig. 9, a significant reduction in the absorption between room and cryogenic temperature is observed: 35 and 45 % between the highest and lowest temperatures for the 450 and 300 °C heat treated samples, respectively. The change in absorption may be due to the semiconductor nature of aSi where there is a considerable amount of free carriers present at room temperature, which accounts for a higher absorption and the significant reduction, as these free carriers are progressively frozen out when lowering temperature.

## III. RAMAN SPECTROSCOPY

Raman spectroscopy provides information about the composition and structure of a material [27]. Figure 10 (a) shows a measurement of the Raman spectrum of the aSi single layer as deposited (blue) and a Raman spectrum of (hydrogenated) aSi from literature (grey) [28]. The measurement shows the characteristic shape of aSi. Figure 10 (b) shows a measurement of the Raman spectrum of the aSi single layer after heat treatment at 450 °C compared to a Raman spectrum from literature for cSi (black dots) in (111) orientation. The Raman spectrum of the aSi single layer after heat treatment at 1200 °C is shown in Fig. 10 (c). For 450 ° annealing temperature (where the minimum optical absorption was observed), the aSi has clearly started to develop some cSi Raman features, indicating that a structural re-orientation towards a crystalline state has begun. This might be related to the absorption reduction. For heat treatment at higher temperatures, the crystalline features in the spectra become more distinct.

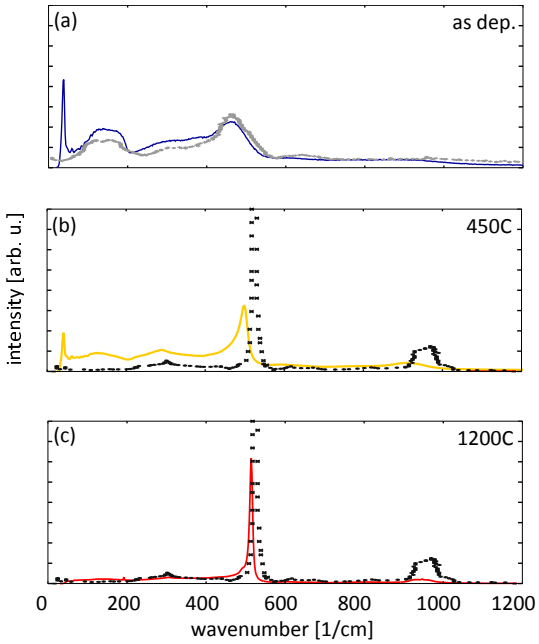


FIG. 10. Raman spectrum measured on the aSi single layer as deposited (blue line, (a)), and after heat treatment at 450 °C (yellow line, (b)) and to 1200 °C (red line, (c)). The grey line in (a) shows literature data for aSi, the black dots in (b) and (c) show literature data for cSi [28].

## IV. SUMMARY AND DISCUSSION

In this paper, measurements of the optical absorption of an aSi single layer (500 nm) coating and an aSi/$SiO_2$ (112 nm aSi, 267 nm $SiO_2$) bilayer coating at wavelengths of 1550 and 1064 nm are presented. Based on reflectivity measurements, the EFI in the aSi layers was estimated and used to scale the measured absorption to a QWL. For heat treatment at up to 500 °C the absorption at 1064 nm is approximately a factor of 3 higher than at 1550 nm. For higher temperatures the difference becomes less significant. It was found that heat treatment can significantly reduce the absorption of IBS aSi coatings. The optimal temperature was shown to be 450 °C, at which the absorption for the aSi single layer shows a minimum corresponding to 755 ppm for a QWL at 1550 nm, while it is 1430 ppm for the bilayer. The absorption of coatings heat treated in air and in vacuum is in good agreement. It was shown that the heating time does not affect the absorption at 1550 nm for an 450 °C heat treated bilayer, which was found to be homogeneously absorbing at a level of 2640 ppm with a standard deviation of 227 ppm over an area of 4 mm × 4 mm. For the aSi single layer, which was heat treated at 450 °C, non-linear effects caused by two photon absorption are shown to be not relevant at 1550 nm in the intensity range used for the measurements and for the intensity range of interest for future GWDs. Temperature dependent measurements have shown that cooling to a temperature of 30 K further reduces the optical absorption at 1550 nm of the aSi based coatings by up to 45 %.

For GWDs, coatings deposited using IBS (such as investigated in this work) are used, because of low scattering, and the ability to coat large substrates with high homogeneity. The absorption for an HR coating based on the IBS aSi single layer results, at the optimum heat treatment temperature, is comparable to previous measurements on an aSi/$SiO_2$ HR coating which was deposited via ion plating showing an absorption of approximately 1000 ppm at 1550 nm [16]. The IBS bilayer absorption is approximately a factor of two higher, but more similar to a multilayer and therefore more comparable to an actual HR coating. Consequently, using IBS aSi (fabricated by ATF and optimally annealed) in an HR coating would mean a factor of two increase in absorption compared to an ion plating coating. Cooling the IBS coating to a cryogenic temperature would almost compensate for the absorption increase, but possibly the absorption of ion plating coatings would also further decrease with cooling.

In conclusion, despite very high absorption in as-deposited coatings, IBS aSi shows some promise for significant absorption reduction through heat treatment and operation at cryogenic temperature. At 20 K, the ATF coatings (assuming no further degradation of absorption in a multi-layer stack with many interfaces in comparison to a bilayer) could provide a thermal noise reduction of 25 % for an absorption of 8.5 ppm when used in a multi-material coating design [17]. Ion plating aSi coatings may also merit further study.

## V. ACKNOWLEDGMENTS

We are grateful for additional financial support from STFC (ST/L000946/1) and the University of Glasgow. I. W. M. is supported by a Royal Society Research Fellowship. S. R. holds a Royal Society Wolfson Research Merit award. We are grateful to the International Max Planck Partnership for Measurement and Observation at the Quantum Limit for support, and we thank our colleagues in the LSC and VIRGO collaborations and within SUPA for their interest in this work. Co-authors at Stanford University are grateful to the NSF for financial support under Grant No. PHYS-1404430.

This paper has LIGO Document number LIGO-P1500257.

[1] B. P. Abbott et al., Observation of Gravitational Waves from a Binary Black Hole Merger, Phys. Rev. Lett. 116, 061102 (2016)

[2] R. Adhikari et al., LIGO III Blue ConceptLIGO, Technical Document LIGO-G1200573, dcc.ligo.org/LIGO-G1200573-v1/public (2012)

[3] M. Abernathy et al., Einstein gravitational wave Telescope (ET) conceptual design study, ET-0106C-10, https://tds.ego-gw.it/ql/?c=7954 (2011)

[4] S Hild, S Chelkowski, A Freise, J Franc, N Morgado, R Flaminio, and R DeSalvo, A xylophone configuration for a third–generation gravitational wave detector, Classical Quantum Gravity **27**, 015003 (2010)

[5] M. E. Fine, H. van Duyne, and N. T. Kenney, Low–Temperature Internal Friction and Elasticity Effects in Vitreous Silica, J. Appl. Phys. **25** 402–5 (1954)

[6] R. Nawrodt et al., High mechanical Q-factor measurements on silicon bulk samples, Journal of Physics: Conference Series **122**, 012008 (2008)

[7] D. F. McGuigan, C. C. Lam, R. Q. Gram, A. W. Hoffman, D. H. Douglass, H. W. Gutche, Measurements of the mechanical Q of single-crystal silicon at low temperatures, Journal of Low Temperature Physics **30**, 624–629 (1978)

[8] S. Rowan, R. L. Byer, M. M. Fejer, R. Route, G. Cagnoli, D. R. M. Crooks, J. Hough, P. H. Sneddon, W. Winkler, Test mass materials for a new generation of gravitational wave detectors, Proceedings of SPIE **4856**, 292–297 (2003)

[9] W. Winkler, K. Danzmann, A. Rüdiger, and R. Schilling, Heating by optical absorption and the performance of interferometric gravitational-wave detectors, Physical Review A **44**, 7022–7036 (1991)

[10] M. J. Keevers, and M. A. Green, Absorption edge of silicon from solar cell spectral response measurements, Appl. Phys. Lett. **66**, 174–176 (1995)

[11] J. Degallaix, R. Flaminio, D. Forest, M. Granata, C. Michel, L. Pinard, T. Bertrand, G. Cagnoli, Bulk optical absorption of high resistivity silicon at 1550 nm, Optics Letter **38**, 2047–2049 (2013)

[12] I. W. Martin et al., Low temperature mechanical dissipation of an ion-beam sputtered silica film, Classical Quantum Gravity **31**, 035019 (2014)

[13] Iain W. Martin et al., Comparison of the temperature dependence of the mechanical dissipation in thin films of $Ta_2O_5$ and $Ta_2O_5$ doped with $TiO_2$, Classical Quantum Gravity **26**, 155012 (2009)

[14] Gregory M. Harry et al., "Thermal noise in interferometric gravitational wave detectors due to dielectric optical coatings", Class. Quantum Grav. **19**, 897–917 (2002)

[15] X. Liu, C. L. Spiel, R. D. Merithew, R. O. Pohl, B. P. Nelson, Q. Wang, R. S. Crandall, Internal friction of amorphous and nanocrystalline silicon at low temperatures, Materials Science and Engineering A **442** 307–313, (2006)

[16] J. Steinlechner, A. Khalaidovski, and R. Schnabel, Optical absorption measurement at 1550 nm on a highly-reflective $Si/SiO_2$ coating stack, Classical Quantum Gravity **31**, 105005 (2014)

[17] J. Steinlechner, I. W. Martin, C. Krueger, J. Hough, S. Rowan, and R. Schnabel, Thermal Noise Reduction and Absorption Optimisation via Multi-Material Coatings, Phys. Rev. D **91** 042001 (2015)

[18] W. Yam, S. Gras, and M. Evans, Multimaterial coatings with reduced thermal , Phys. Rev. D **91**, 042002 (2015)

[19] P. G. Murray, I. W. Martin, M. R. Abernathy, K. Craig, J. Hough, T. Pershing, S. Penn, R. Robie, S. Rowan, Ion-beam sputtered amorphous silicon films for cryogenic precision measurement systems, accepted for publication in Phys. Rev. D (2015)

[20] ATFilms, USA, http://www.atf-ppc.com

[21] A. L. Alexandrovski, M. M. Fejer, A. Markosyan, and R. Route, Photothermal common-path interferometry (PCI): new developments, Proc. SPIE 7193, Solid State Lasers XVIII: Technology and Devices **71930D** doi: 10.1117/12.814813 (2009)

[22] J. Steinlechner, I. W. Martin, A. Bell, G. Cole, J. Hough, S. Penn, S. Rowan, S. Steinlechner, Mapping the Optical Absorption of a Substrate-Transferred Crystalline AlGaAs Coating at 1.5 $\mu$m, Accepted for publication in Classical and Quantum Gravity **32**, 105008 (2015)

[23] https://github.com/sestei/dielectric

[24] www.newport.com

[25] H. W. Pan, S. J. Wang, L. C. Kuo, S. Chao, M. Principe, I. M. Pinto, R. DeSalvo, Thickness-dependent crystallization on thermal anneal for titania/silica nm-layer composites deposited by ion beam sputter method, Opt Express. **22**, 29847–54 (2014)

[26] Q. Lin, O. J. Painter, and G. P. Agrawal, Nonlinear optical phenomena in silicon waveguides: Modeling and applications, Optics Express **15**, 16604–16644 (2007)

[27] N. Colthub, L. Daly, and S. Wiberley, Introduction to Infrared and Raman Spectroscopy, Academic Press Inc., London

[28] A. Zwick and R. Carles, Multiple-order Raman scattering in crystalline and amorphous silicon, Phys. Rev. B **48**, 9 (1993)